Column Water Vapor Content in Clear and Cloudy Skies

DIAN J. GAFFEN AND WILLIAM P. ELLIOTT

NOAA/ERL, Air Resources Laboratory, Silver Spring, Maryland

(Manuscript received 30 January 1993, in final form 14 June 1993)

ABSTRACT

With radiosonde data from 15 Northern Hemisphere stations, surface-to-400-mb column water vapor is computed from daytime soundings for 1988–1990. On the basis of simultaneous surface visual cloud observations, the data are categorized according to sky-cover amount. Climatological column water vapor content in clear skies is shown to be significantly lower than in cloudy skies. Column water vapor content in tropical regions varies only slightly with cloud cover, but at midlatitude stations, particularly in winter, clear-sky values are much lower. The variation in column water content with cloud cover is not simply due to variations in atmospheric temperature, since the increase in water vapor with cloud cover is generally associated with a decrease in daytime temperature. Biases in radiosonde instruments associated with cloudiness do not explain the station-to-station variations in the magnitude of the increase of column water vapor with cloud cover. Statistics are presented that can be used as guidance in estimating the bias in water vapor climatologies based on clear-sky or partly cloudy-sky measurements. These may be helpful in distinguishing the clear- and cloudy-sky greenhouse effects of water vapor.

1. Introduction

It seems obvious that the atmospheric column water vapor content (W) in cloudy skies would typically exceed W in clear skies. Frontal clouds tend to be associated with advection of warm, humid air. Convective clouds transport moisture from the boundary layer into the free atmosphere. However, quantitative estimates of the variation of W with cloud cover are lacking.

This variation has important ramifications for both observational and theoretical climate studies. Satellite methods for retrieving W using infrared and visible (but not microwave) radiation are generally restricted to cloud-free regions (NASA 1991). Climatologies of W based on these observations will be biased toward clear, and presumably drier, skies. One use of W measurements from satellites is to determine the radiation budget of the atmosphere. Assessments of the role of water vapor in both the clear- and cloudy-sky radiation budgets should take into account any climatological differences in W between clear and cloudy skies.

Radiosonde observations are made routinely in all weather and so can be used to assess the clear-sky bias in W, as we present here. Burova (1988) estimated the relationship between cloud cover and W using radiosonde data and found a general increase in W with increasing cloud cover. However, her analysis used radiosonde data from Arctic stations, where humidity measurements are considered poor due to the cold, dry conditions.

The next section outlines the data and methods used. The following section presents variations in both seasonal and annual mean W, $\bar{W}$, as a function of cloud cover and presents estimates of the bias in $\bar{W}$ climatologies that are based on observations limited by cloudiness. Next we discuss the possible effects both of the relationship of W and surface temperature and of radiosonde sensor errors on the bias estimates and summarize our findings on the magnitude of the bias.

2. Data and method

Daily daytime radiosonde observations for the period 1988–1990 from 15 Northern Hemisphere stations (Fig. 1 and Table 1) were used to compute W, the vertical integral of specific humidity, for the surface-to-400-mb layer. The station selections were an attempt to satisfy four requirements: 1) collocation of the radiosonde station with a visual cloud observing station, 2) a distribution that would yield a reasonable latitudinal sampling, 3) a set of stations that use radiosondes equipped with relatively fast-response humidity sensors (carbon hygristors or capacitive thin-film sensors), and 4) a set of stations whose cloud climatologies included enough clear observations to allow an assessment of the difference between clear and cloudy days. As discussed in more detail below, the last requirement could not always be satisfied because in some regions clear skies are rarely observed.

The W integration was performed only if a complete temperature and humidity observation was available

Corresponding author address: Dr. Dian Gaffen, NOAA Air Resources Laboratory, R/E/AR, 1315 East-West Highway, Silver Spring, MD 20910.

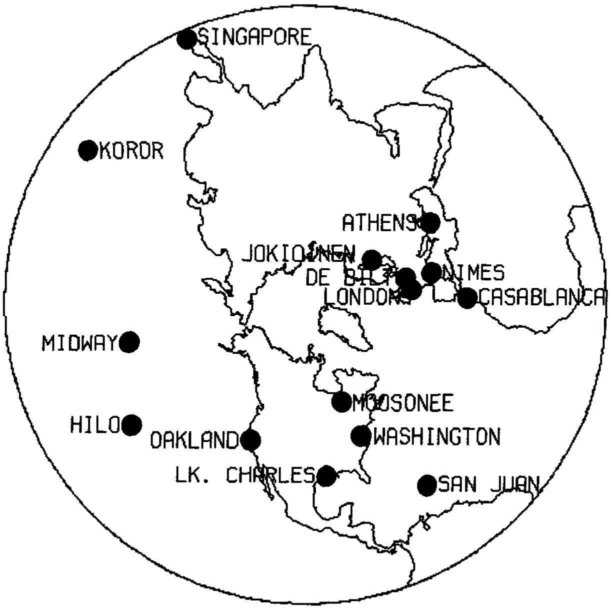

FIG. 1. Station locations.

for the surface and the four mandatory reporting levels at 850, 700, 500, and 400 mb. Data from intermediate "significant" levels were also included. Gross error checking eliminated soundings with unrealistic temperature, dewpoint depression, and surface pressure data. Instrument-type information in the radiosonde reports, combined with historical information on radiosonde instruments obtained from the responsible weather services, indicated that no important changes in instruments were made at these stations during the period analyzed, so we can assume that observed W variations are not due to instrument changes.

Cloud-cover data were visual surface observations for the same stations and at the same times as the radiosonde data, with the single exception that cloud data were not available for Crawley (51°05′N, 00°13′W) so Gatwick Airport, London (51°09′N, 00°11′W), was substituted. We chose daytime data to avoid difficulties associated with visual observations of clouds in darkness (Warren et al. 1986, 1988). Total sky-cover data were archieved in oktas (USAFETC 1986), and we categorized these as clear (CLR), scattered (SCT), broken (BKN), or overcast (OVC). The categorization was based on the WMO "category of cloud amount" code $N_sN_sN_s$ (WMO 1991) where 0 oktas is CLR, 1 to 4 is SCT, 5 to 7 is BKN, and 8 is OVC. Reports of sky obscured or partially obscured (that include fog) were discarded in this analysis. Surface temperature (T) was also obtained from the surface observations.

In categorizing of the sky-cover data, we found a curious distribution of values at the United States–operated stations. (These include Koror, San Juan, Hilo, Midway, Lake Charles, Oakland, and Washington.) At five of the seven stations, the value 5/8 was never reported, and at Koror and Lake Charles, only 1.2% and 0.3%, respectively, of the total number of observations were for 5/8. At Oakland there were no reports of 1/8, 3/8, 4/8, or 6/8 either. The Oakland data are categorical sky-cover reports, in which values of 0, 2, 7, and 8 oktas represent CLR, SCT, BKN, and OVC, respectively. The other station data may be a mixture of categorical and okta-value sky-cover data; in the United States, hourly airways reports are categorical, but synoptic reports, every three hours, are not (N. Lott 1992, personal communication). But that does not explain the complete absence of 5/8. Nor does the fact that U.S. synoptic observations are made in tenths, which must have been converted to okta values.

Only if both radiosonde and sky-cover data were available was a given observation included in the analysis. Complete observations were available 67% to 95% of the total possible days, depending on the station.

The data were sorted according to the four cloud-cover categories and according to season. (Summer was defined as June, July, August, etc.) Seasonal and annual $\bar{W}$ values were computed for each cloud category and for the complete data. Ratios of the seasonal $\bar{W}$ values for CLR, SCT, and BKN skies to $\bar{W}$ for OVC skies were computed as a measure of the effect of cloud cover on $\bar{W}$.

Three additional parameters were computed to quantify the bias in climatological $\bar{W}$ values. The first is

$$B_0 = 1 - \frac{\bar{W}_{\mathrm{CLR}}}{\bar{W}_{\mathrm{ALL}}}. \qquad (1)$$

Here $\bar{W}_{\mathrm{ALL}}$ is the weighted mean of all observations,

$$\bar{W}_{\mathrm{ALL}} = \frac{(N_{\mathrm{CLR}}\bar{W}_{\mathrm{CLR}} + N_{\mathrm{SCT}}\bar{W}_{\mathrm{SCT}} + N_{\mathrm{BKN}}\bar{W}_{\mathrm{BKN}} + N_{\mathrm{OVC}}\bar{W}_{\mathrm{OVC}})}{N_{\mathrm{CLR}} + N_{\mathrm{SCT}} + N_{\mathrm{BKN}} + N_{\mathrm{OVC}}}. \qquad (2)$$

The subscripts refer to the four cloud categories and N is the number of daily samples used to calculate the seasonal mean. The subscript 0 in Eq. (1) indicates that only sky-cover values of 0 oktas are used in the calculating numerator. When expressed as a percentage, B_0 is the percent by which $\bar{W}$ is underestimated when only clear-sky observations are included.

A second bias estimator is

$$B_4 = 1 - \frac{\dfrac{N_{\mathrm{CLR}}\bar{W}_{\mathrm{CLR}} + N_{\mathrm{SCT}}\bar{W}_{\mathrm{SCT}}}{N_{\mathrm{CLR}} + N_{\mathrm{SCT}}}}{\bar{W}_{\mathrm{ALL}}}, \qquad (3)$$

where the subscript 4 indicates that all sky-cover values up to 4/8 are included in the numerator. For an extreme case, we also computed

$$B_7 = 1 - \frac{\dfrac{N_{\mathrm{CLR}}\bar{W}_{\mathrm{CLR}} + N_{\mathrm{SCT}}\bar{W}_{\mathrm{SCT}} + N_{\mathrm{BKN}}\bar{W}_{\mathrm{BKN}}}{N_{\mathrm{CLR}} + N_{\mathrm{SCT}} + N_{\mathrm{BKN}}}}{\bar{W}_{\mathrm{ALL}}}. \qquad (4)$$

TABLE 1. For each station, seasonal and annual mean column water vapor content $\bar{W}$ (kg m^{-2}), for each of four cloud categories (CLR, SCT, BKN, OVC) and without regard to cloudiness (ALL). Following $\bar{W}$ is the number N of observations comprising the mean. If there were no CLR observations, a dash is shown. Stations are arranged in order of increasing latitude, and location and time used are included.

	DJF		MAM		JJA		SON		YEAR	
	$\bar{W}$	N	$\bar{W}$	N	$\bar{W}$	N	$\bar{W}$	N	$\bar{W}$	N
Singapore, Singapore (1°22′N, 103°59′E) 0000 UTC										
CLR	—	0	—	0	—	0	—	0	—	0
SCT	46.4	11	49.8	18	52.5	6	52.0	4	49.5	39
BKN	48.6	145	52.8	129	51.1	148	52.0	152	51.1	574
OVC	56.0	19	57.9	14	54.4	21	55.0	32	55.5	86
ALL	49.3	175	52.9	161	51.5	175	52.5	188	51.6	699
Koror, Palau Islands (7°20′N, 134°29′E) 0000 UTC										
CLR	—	0	—	0	—	0	—	0	—	0
SCT	42.0	53	46.7	53	52.7	42	50.9	48	47.7	196
BKN	46.2	54	53.2	38	55.0	55	52.8	42	51.7	189
OVC	52.1	96	54.4	81	56.2	92	55.3	98	54.5	367
ALL	47.9	203	51.8	172	55.1	189	53.6	188	52.0	752
San Juan, Puerto Rico, U.S.A. (18°26′N, 66°00′W) 1200 UTC										
CLR	27.3	8	31.2	14	40.1	6	38.0	5	32.9	33
SCT	32.2	127	34.2	123	41.3	143	42.0	139	37.7	532
BKN	35.5	88	37.0	51	46.1	76	47.7	64	41.5	279
OVC	35.7	13	41.8	19	48.9	25	49.4	18	44.9	75
ALL	33.4	236	35.4	207	43.5	250	44.1	226	39.3	919
Hilo, Hawaii, U.S.A. (19°43′N, 155°04′W) 0000 UTC										
CLR	34.2	1	—	0	—	0	—	0	34.2	1
SCT	28.4	90	28.3	68	30.9	81	34.1	68	30.3	307
BKN	31.8	61	32.6	75	33.8	93	38.4	94	34.5	323
OVC	38.0	76	35.8	75	38.7	53	43.4	62	38.8	266
ALL	32.5	228	32.4	218	33.9	227	38.5	224	34.3	897
Midway Island (28°13′N, 177°22′W) 0000 UTC										
CLR	21.5	3	20.3	5	—	0	—	0	20.8	8
SCT	20.2	109	22.4	114	34.1	174	32.1	140	28.3	537
BKN	23.6	107	27.8	87	41.4	72	34.1	93	30.9	359
OVC	32.0	25	34.4	25	43.0	4	39.2	14	35.0	68
ALL	22.9	244	25.7	231	36.4	250	33.3	247	29.7	972
Lake Charles, Louisiana, U.S.A. (30°07′N, 93°13′W) 1200 UTC										
CLR	8.9	48	14.1	34	32.5	14	18.7	90	16.4	186
SCT	13.6	16	20.6	34	42.3	82	32.3	73	32.9	205
BKN	15.9	13	23.0	22	46.7	41	32.9	34	34.0	110
OVC	25.2	103	26.8	66	51.6	37	36.2	42	31.4	248
ALL	19.1	180	22.2	156	44.5	174	28.0	239	28.5	749
Casablanca, Morocco (33°34′N, 7°40′W) 1200 UTC										
CLR	13.3	36	18.0	16	27.7	48	23.5	26	21.5	126
SCT	15.6	56	18.2	58	28.1	91	25.7	52	22.7	257
BKN	18.5	112	18.3	131	28.0	65	26.4	118	22.1	426
OVC	23.7	14	21.8	10	34.4	6	28.7	18	26.5	48
ALL	17.2	218	18.4	215	28.2	210	26.1	214	22.4	857
Oakland, California, U.S.A. (37°44′N, 122°13′W) 0000 UTC										
CLR	7.7	73	11.1	66	17.1	158	14.6	126	13.8	423
SCT	10.7	53	13.0	70	21.4	56	15.7	57	15.1	236
BKN	12.3	59	15.2	49	22.1	26	18.2	41	15.9	175
OVC	16.0	39	21.2	49	18.7	11	19.0	33	18.9	132
ALL	11.1	224	14.6	234	18.7	251	16.0	257	15.2	966
Athens, Greece (37°54′N, 23°44′E) 1200 UTC										
CLR	9.5	25	11.4	21	20.2	90	16.6	25	16.8	161
SCT	10.6	84	14.1	102	22.6	132	18.8	135	17.3	453
BKN	13.9	99	16.0	84	24.5	34	21.3	77	17.7	294
OVC	18.0	20	17.3	27	24.4	4	24.6	20	20.0	71
ALL	12.6	228	14.9	234	22.0	260	19.8	257	17.5	979
Washington, Dulles Airport, U.S.A. (38°57′N, 77°27′W) 1200 UTC										
CLR	5.4	25	8.4	31	27.6	40	14.5	33	15.3	129
SCT	7.1	53	11.2	48	28.9	71	14.2	71	16.3	243
BKN	7.2	35	16.9	31	35.0	50	16.0	39	20.3	155
OVC	15.8	90	21.2	97	38.9	82	29.2	73	25.8	342
ALL	10.8	203	16.3	207	33.3	243	19.7	216	20.6	869
Nimes, France (43°52′N, 4°24′E) 1200 UTC										
CLR	8.2	42	12.5	22	20.1	41	13.6	31	13.7	136
SCT	10.3	54	13.8	70	24.0	109	16.6	83	17.5	316
BKN	14.3	76	18.3	91	27.1	61	21.3	90	19.9	318
OVC	17.9	37	20.9	28	32.9	6	26.5	28	22.1	99
ALL	12.7	209	16.6	211	24.4	217	19.2	232	18.3	869
London, Crawley, U.K. (51°09′N, 0°11′W) 1200 UTC										
CLR	4.4	1	13.7	7	17.4	5	14.3	4	14.4	17
SCT	7.7	39	10.9	63	18.5	81	11.9	68	13.1	251
BKN	10.6	92	12.3	110	18.7	146	16.2	144	15.0	492
OVC	14.1	96	14.6	48	23.3	40	21.8	49	17.4	233
ALL	11.6	228	12.4	228	19.3	272	16.1	265	15.1	993
Moosonee, Canada (51°16′N, 80°39′W) 1200 UTC										
CLR	2.2	59	4.6	32	21.9	9	14.5	3	5.0	103
SCT	3.0	54	6.1	52	19.4	79	9.3	61	10.5	246
BKN	3.2	40	9.4	40	19.9	87	12.0	60	13.0	227
OVC	5.6	82	11.0	98	24.1	81	13.1	124	13.3	385
ALL	3.7	235	8.7	222	21.2	256	11.9	248	11.6	961
De Bilt, the Netherlands (52°06′N, 5°11′E) 1200 UTC										
CLR	7.7	5	10.7	15	21.7	6	15.4	13	13.6	39
SCT	8.2	27	11.2	66	21.4	62	13.6	46	14.5	201
BKN	10.9	113	13.0	104	21.1	141	16.6	132	15.8	490
OVC	14.7	116	16.6	56	26.1	64	22.5	76	19.3	312
ALL	12.3	261	13.2	241	22.4	273	17.7	267	16.5	1042
Jokioinen, Finland (60°49′N, 23°30′E) 1200 UTC										
CLR	2.5	8	6.5	5	—	0	5.4	5	4.4	18
SCT	4.5	31	8.2	57	17.3	67	8.7	53	10.7	208
BKN	6.2	60	9.5	100	20.6	140	11.2	103	13.3	403
OVC	9.5	151	11.7	89	25.2	49	14.3	96	13.2	385
ALL	7.9	250	9.9	251	20.6	256	11.7	257	12.6	1014

The probability of a radiosonde passing through a cloud can be estimated by the product of the probability of encountering a cloud for a given cloud-cover category and the probability of occurrence of that category, summed over all categories. Using the three years of sky-cover data, we computed

$$P = \sum_{k=0}^{8} \frac{k}{8} \frac{n_k}{N}, \qquad (5)$$

where the index k is the sky-cover amount, in oktas, n_k is the number of observations per category, and N is the total number of observations.

3. Results

a. *Cloud-cover climatology*

While the focus of this study is not the climatology of cloud cover, a summary of the station cloud climatologies provides a basis for understanding the cloud effects on $\bar{W}$. Note, however, that the once-daily observations are always daytime, and that local cloud climatology is likely to vary diurnally (Warren et al. 1986, 1988). In addition, because radiosondes are launched at 0000 and 1200 UTC, we are sampling different local times at each station—near noon in Europe and in the Pacific and morning or evening in Asia and North America.

Table 1 gives the number of observations in each category for each station, and Table 2 shows the estimated probability P that the radiosondes passed through clouds. At the five stations closest to the equator, clear-sky observations are quite rare. At Singapore and Koror, not a single 0000 UTC CLR report was made in three years, and at Puerto Rico, the tropical station with the greatest number of clear days, fewer than 4% of the observations were CLR (Table 1). The associated P values are generally greater than 0.5, meaning that a radiosonde is more likely than not to pass through a cloud (Table 2). The frequent occurrence of cumulus convection and associated cirrus blow-off in the tropics probably accounts for these statistics. The midlatitude stations are decidedly sunnier. (In fact, they were selected because of their relatively high frequency of CLR observations, our purpose being to quantify the clear-sky bias.) Four of the six stations between 30° and 50°N have 15% to 16% CLR observations, while Oakland and Lake Charles have 44% and 25% CLR observations, respectively. The high fraction at Oakland is probably due to a combination of the effect of the Pacific high pressure system, creating strong subsidence in summer and fall, and the 0000 UTC observation time (about 1600 local time), which is late enough in the day that most advection fog from the Pacific Ocean will have been dissipated. On the other hand, it may be an artifact of the lack of observations of 1/8 sky cover at Oakland, so that more observations are for 0/8 than is realistic.

The midlatitude stations exhibit much more seasonality in their cloud regimes, as measured by both N_{CLR} and P. Summer is generally the sunniest season, and P values are lowest then. The stations with Mediterranean climates, Casablanca, Nimes, and Athens, have summertime P values between 0.2 and 0.4, which suggests that radiosondes are unlikely to pass through clouds at those stations in summer. Oakland P values are also in this range, but are not considered meaningful because of the data limitations mentioned above. (This overrepresentation of stations with Mediterranean climates may bias our assessment of the cloudiness in typical midlatitude regions toward a less cloudy climatology.)

At the four most northerly stations, cloudy skies again dominate. At the northern European stations, London, de Bilt, and Jokioinen, which are influenced by the Atlantic Ocean, fewer than 4% of the 1200 UTC observations are CLR, and at Moosonee the fraction is 11%. At these stations, P typically exceeds 0.6 in all seasons.

At most of the stations analyzed in this study, the most frequently reported category was either SCT or BKN, with the exceptions of Koror, Lake Charles, Washington Dulles, Moosonee (most frequently OVC), and Oakland (most frequently CLR). Indeed, on the basis of global visual cloud observations, Warren et al. (1986) find that, on global average, land areas report completely clear skies with a frequency of about 18%. For ocean areas, the global average frequency is only 3% (Warren et al. 1988). Using satellite observations, Rossow and Lacis (1990) also find ocean regions generally have larger cloud cover than continental regions.

b. *Column water vapor content*

As is well known (e.g., Peixoto and Oort 1992), and as these data confirm, the most prominent feature of the climatology of W is its decrease with latitude. Our limited station set shows a gradient from more than 50 kg m^{-2} at Singapore, near the equator, to about 13 kg m^{-2} over Finland (Table 1) on annual average. Categorization of the data by season and cloud cover evinces two sources of temporal variability in the station data. The first is the seasonal cycle in $\bar{W}$, which can be large, especially at higher-latitude stations where summertime $\bar{W}$ can be two to six times the wintertime values. At most of our 15 stations, $\bar{W}$ reaches a maximum in summer. The exceptions are Singapore, where the maximum is in spring, and San Juan and Hilo, where it is in fall. At these stations the annual cycles in $\bar{W}$ are small (maximum seasonal $\bar{W}$ values are at most 12% greater than the annual mean).

A second source of variability in $\bar{W}$, and the focus of this study, is cloud cover. As expected, $\bar{W}$ increases progressively with increasing cloud cover for almost every season at all 15 stations (Table 1). In a few cases,

TABLE 2. The ratios of $\bar{W}$ for CLR, SCT, and BKN sites to $\bar{W}$ for OVC, for each station and season. The bias indices, B_0, B_4, and B_7 (dimensionless), and the probability of a sounding passing through a cloud, P, as defined in the text, are also shown. (No P values are given for Oakland, where the categorical cloud data made this computation dubious.) A dash is shown when there were no CLR observations. W ratios and B values based on fewer than 10 observations of CLR (or CLR and SCT combined), and W ratios based on fewer than 10 OVC observations, are marked with an asterisk (*) and a pound sign (#), respectively.

	DJF	MAM	JJA	SON
Singapore, Singapore				
CLR/OVC	—	—	—	—
SCT/OVC	0.83	0.86	0.96*	0.94*
BKN/OVC	0.87	0.91	0.94	0.95
B_0	—	—	—	—
B_4	0.06	0.06	−0.02*	0.01*
B_7	0.02	0.01	0.01	0.01
P	0.83	0.81	0.85	0.87
Koror, Palau Islands				
CLR/OVC	—	—	—	—
SCT/OVC	0.81	0.86	0.94	0.92
BKN/OVC	0.89	0.98	0.98	0.95
B_0	—	—	—	—
B_4	0.12	0.10	0.04	0.05
B_7	0.08	0.05	0.02	0.03
P	0.78	0.74	0.79	0.77
San Juan, Puerto Rico, U.S.A.				
CLR/OVC	0.76*	0.75	0.82*	0.77*
SCT/OVC	0.90	0.82	0.85	0.85
BKN/OVC	0.99	0.88	0.94	0.97
B_0	0.18*	0.12	0.08*	0.14*
B_4	0.05	0.04	0.05	0.05
B_7	0.00	0.02	0.01	0.01
P	0.50	0.45	0.51	0.48
Hilo, Hawaii, U.S.A.				
CLR/OVC	0.90*	—	—	—
SCT/OVC	0.75	0.79	0.80	0.79
BKN/OVC	0.84	0.91	0.87	0.88
B_0	−0.05*	—	—	—
B_4	0.13	0.13	0.09	0.11
B_7	0.08	0.06	0.04	0.05
P	0.66	0.71	0.67	0.71
Midway Island				
CLR/OVC	0.67*	0.59*	—	—
SCT/OVC	0.63	0.65	0.79#	0.82
BKN/OVC	0.74	0.81	0.96#	0.87
B_0	0.06*	0.21*	—	—
B_4	0.12	0.13	0.06	0.03
B_7	0.05	0.04	0.00	0.01
P	0.58	0.55	0.45	0.52
Lake Charles, Louisiana, U.S.A.				
CLR/OVC	0.35	0.53	0.63	0.52
SCT/OVC	0.54	0.77	0.82	0.89
BKN/OVC	0.63	0.86	0.90	0.91
B_0	0.54	0.36	0.27	0.33
B_4	0.47	0.22	0.08	0.11
B_7	0.42	0.15	0.04	0.06
P	0.65	0.58	0.52	0.35
Casablanca, Morocco				
CLR/OVC	0.56	0.83	0.81	0.82
SCT/OVC	0.66	0.83	0.82	0.90
BKN/OVC	0.78	0.84	0.82	0.92
B_0	0.23	0.02	0.02	0.10
B_4	0.15	0.01	0.01	0.04
B_7	0.03	0.01	0.01	0.01
P	0.55	0.62	0.41	0.60
Oakland, California, U.S.A.				
CLR/OVC	0.48	0.52	0.92	0.77
SCT/OVC	0.67	0.61	1.15	0.82
BKN/OVC	0.77	0.72	1.18	0.96
B_0	0.30	0.24	0.08	0.09
B_4	0.19	0.17	0.02	0.07
B_7	0.09	0.12	0.00	0.03
Athens, Greece				
CLR/OVC	0.53	0.65	0.83	0.67
SCT/OVC	0.59	0.82	0.93	0.76
BKN/OVC	0.77	0.92	1.00	0.86
B_0	0.24	0.24	0.08	0.16
B_4	0.18	0.09	0.02	0.07
B_7	0.04	0.02	0.00	0.02
P	0.54	0.50	0.22	0.45
Washington, Dulles Airport, U.S.A.				
CLR/OVC	0.34	0.40	0.71	0.50
SCT/OVC	0.45	0.53	0.74	0.49
BKN/OVC	0.45	0.79	0.90	0.55
B_0	0.50	0.48	0.17	0.26
B_4	0.39	0.38	0.15	0.27
B_7	0.37	0.26	0.09	0.25
P	0.64	0.64	0.58	0.56
Nimes, France				
CLR/OVC	0.45	0.60	0.61#	0.51
SCT/OVC	0.58	0.66	0.73#	0.63
BKN/OVC	0.80	0.88	0.82#	0.80
B_0	0.36	0.24	0.18	0.29
B_4	0.26	0.19	0.06	0.18
B_7	0.09	0.04	0.01	0.05
P	0.54	0.57	0.37	0.52
London, Crawley, U.K.				
CLR/OVC	0.31*	0.94*	0.75*	0.66*
SCT/OVC	0.54	0.75	0.80	0.55
BKN/OVC	0.75	0.84	0.80	0.74
B_0	0.62*	−0.10*	0.10*	0.11*
B_4	0.34	0.10	0.04	0.25
B_7	0.16	0.05	0.04	0.08
P	0.80	0.67	0.66	0.70
Moosonee, Canada				
CLR/OVC	0.38	0.42	0.91*	1.11*
SCT/OVC	0.53	0.55	0.80	0.71
BKN/OVC	0.57	0.86	0.82	0.92
B_0	0.42	0.54	−0.04*	−0.22*
B_4	0.32	0.36	0.07	0.20
B_7	0.27	0.21	0.06	0.10
P	0.53	0.64	0.67	0.75
De Bilt, the Netherlands				
CLR/OVC	0.52*	0.64	0.83*	0.69
SCT/OVC	0.56	0.67	0.82	0.60
BKN/OVC	0.74	0.78	0.81	0.74
B_0	0.37*	0.19	0.03*	0.13
B_4	0.33	0.16	0.04	0.21
B_7	0.16	0.08	0.05	0.11
P	0.84	0.66	0.72	0.73
Jokioinen, Finland				
CLR/OVC	0.27*	0.55*	—	0.38*
SCT/OVC	0.47	0.71	0.69	0.61
BKN/OVC	0.65	0.81	0.82	0.78
B_0	0.68*	0.35*	—	0.54*
B_4	0.48	0.18	0.16	0.28
B_7	0.32	0.10	0.05	0.13
P	0.83	0.73	0.71	0.75

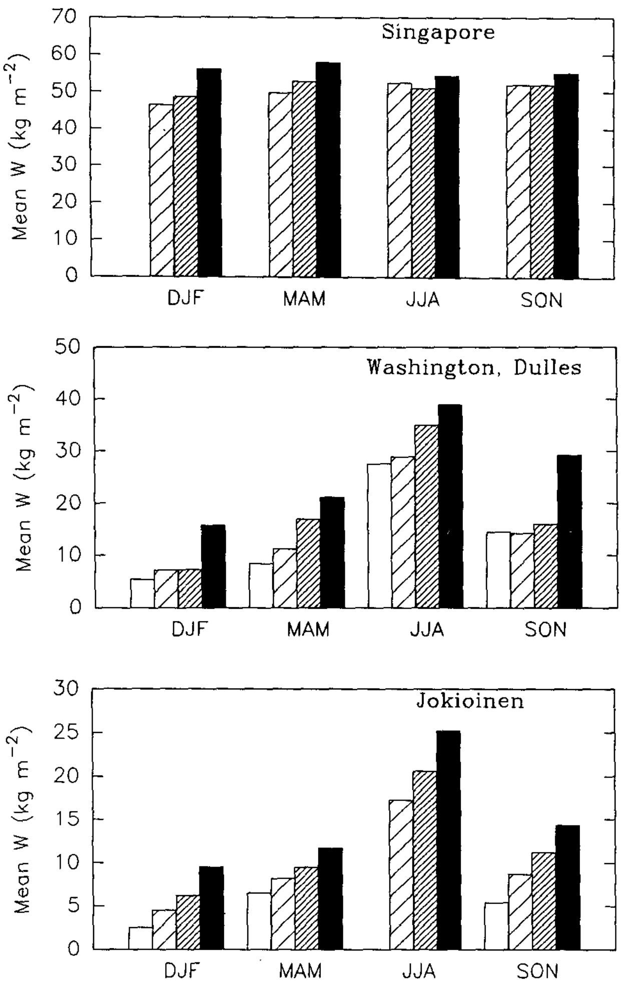

FIG. 2. Mean seasonal column water content, $\bar{W}$, based on radiosonde data for 1988–1990, at Singapore, Washington Dulles, and Jokioinen, categorized by total sky cover. In each histogram, the open, coarsely hatched, finely hatched, and filled bars are for CLR, SCT, BKN, and OVC observations, respectively.

$\bar{W}$ is greater for a less cloudy category than for the next cloudiest, but in each of these cases the difference was not statistically significant at the 95% confidence level, based on a t test, mainly because there were very few observations in at least one of the categories.

The statistics in Table 2 provide a summary, by season, of the relationship between cloud cover and $\bar{W}$. At the tropical stations, the ratios of $\bar{W}$ for each other category to $\bar{W}_{OVC}$ are large, generally greater than 0.8, although $\bar{W}_{CLR}/\bar{W}_{OVC}$ is not meaningful at these stations where N_{CLR} is negligibly small. As shown for the example of Singapore (Fig. 2), $\bar{W}$ increases with cloud cover, but only slightly, and the difference in $\bar{W}$ between cloud categories is a small fraction of the mean value.

The bias estimators, B_0, B_4, and B_7 are small in the tropics (Table 2). Although B_0 tends not to be meaningful because of the paucity of CLR observations, it is generally the case that

$$B_0 > B_4 > B_7 \qquad (6)$$

as one might expect. Values tend to range from 0% to 15% with little seasonal variation.

This result may be explained by two attributes of the tropical atmosphere, the influence of the ocean and the prevalence of high cirrus clouds. Boundary-layer humidity is typically high and temperature variations are typically small at tropical island locations, so that even without clouds the atmosphere is not far from saturation. Since W is influenced strongly by the water content of the boundary layer, the association of W with clouds above will be less than in regions where boundary-layer humidity is more closely linked with cloud cover.

In our sample of stations, we find that a greater fraction of OVC observations at low-latitude stations is high cirrus than at higher latitudes. We examined the cloud ceiling height data available with the cloud cover data. Figure 3 shows the fraction of observations of OVC skies accompanied by an observation of cloud ceiling above 5 km. That this fraction is largest closest to the equator suggests that high cirrus, with no low or midlevel clouds, is more prevalent in the tropics. Such OVC skies would have little impact on surface to

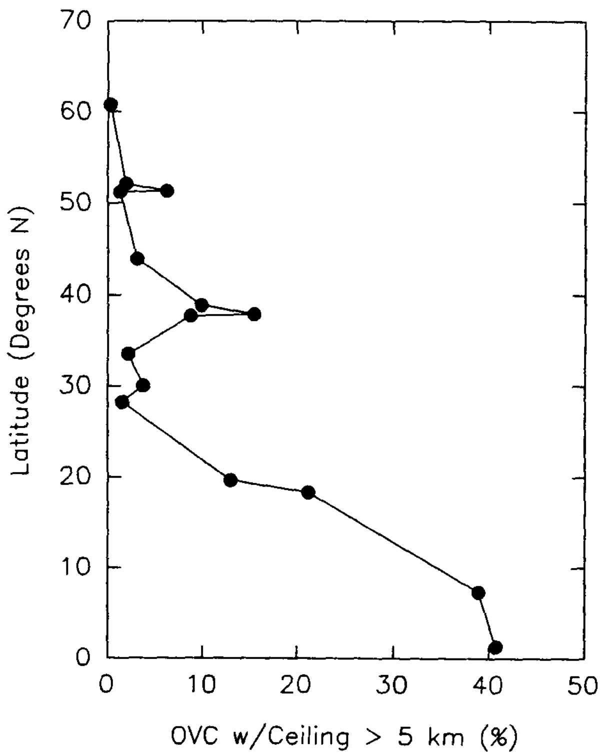

FIG. 3. Fraction of overcast cloud cover observations paired with observations of ceiling heights greater than 5 km for each station, as a function of station latitude.

400-mb W as compared with, for example, a deck of low stratus. Therefore, climatologies limited by cloud cover will only slightly underestimate $\bar{W}$ in the tropics; however, if CLR skies are required, opportunities to sample the tropical atmosphere will be rare.

At higher latitudes, the $\bar{W}$ ratios are considerably smaller, and B values considerably larger, than in the tropics, and they have a distinct seasonal cycle, with a maximum bias generally in winter. The ratio of extremes, $\bar{W}_{CLR}/\bar{W}_{OVC}$, is as small as 0.3 in winter at some stations, but summertime values generally exceed 0.6. At Washington Dulles, and Jokioinen, for example, there is a clear tendency for $\bar{W}$ to increase with cloud cover (Fig. 2).

The B values follow suit. Outside the tropics, wintertime values of B_0 range from about 20% to 60%, and summertime values are between about 0% and 50%. There is a general tendency for the bias to decrease (B approaches 0) when more cloud cover categories are included in the estimate, and summertime B_7 values are less than 10% at most stations.

The generally higher wintertime midlatitude B values might well be due to the different airmass types that cause cloudy conditions in northern latitudes. Clear skies are associated with cold dry air masses, whose ability to hold water vapor is limited by their low temperature, whereas cloudy skies might be associated with warmer, maritime air masses, with a larger vapor-carrying capacity. Our finding that there is a larger variation of W between clear and cloudy skies in midlatitudes and in winter appears consistent with the satellite-based finding that tropical clouds and summertime clouds are optically thinner than midlatitude clouds and wintertime clouds (Tselioudis et al. 1992).

The general tendency for the B estimates to decrease with increasing $\bar{W}$ and for Eq. (6) to apply are shown in Fig. 4, a plot of all the seasonal station values. There are fewer B_0 values than B_4 or B_7 values at high $\bar{W}$, because points were plotted only if 10 or more observations were used to compute the B value and there is a paucity of CLR observations. While there is a fair amount of scatter in the data, an initial rapid decrease in B with increasing $\bar{W}$, due to the seasonal variation in both at midlatitudes, and the leveling-off of B at high values of $\bar{W}$ at the warmest locations and seasons are evident.

When the B_0, B_4, or B_7 values in Fig. 4 are examined separately, a few patterns emerge. The large scatter in B_0 suggests that $\bar{W}$ climatologies based only on clear-sky data will underestimate the true mean by up to 50%, but the exact magnitude is difficult to determine. The initial rapid fall in B_4 followed by a leveling-off at about 5% to 10% for $\bar{W}$ above about 25 kg m^{-2}, suggests that in moist regions if both CLR- and SCT-sky W observations are available the bias in $\bar{W}$ should be small. This bias will be even lower if BKN-sky data

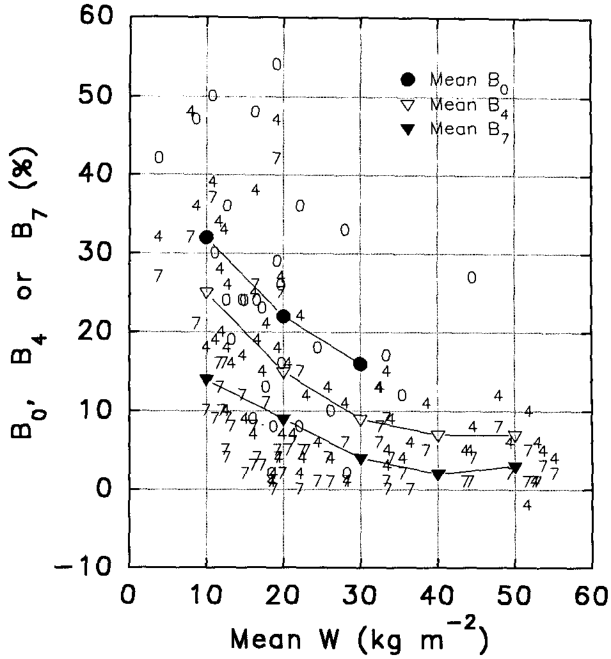

FIG. 4. For each station and season, the indices B_0, B_4, and B_7 (plotted as 0, 4, and 7, respectively), as defined in the text, are plotted versus seasonal mean column water vapor content, $\bar{W}$. Binned mean values ($\bar{B}_0$, $\bar{B}_4$, and $\bar{B}_7$) are shown as symbols.

are included, but B_7 values are still quite variable for $\bar{W}$ below 20 kg m^{-2}.

To provide guidance for estimating biases, Fig. 4 also shows mean values of B_0, B_4, and B_7 ($\bar{B}_0$, $\bar{B}_4$, and $\bar{B}_7$), at 10 kg m^{-2} increments, computed by binning the seasonal station values from 5 to 14.9 kg m^{-2}, 15 to 24.9 kg m^{-2}, etc. No $\bar{B}_0$ values are given for $\bar{W}$ > 30 kg m^{-2} because there are so few data points. A further interpretation of these data is given by Fig. 5, where the products of each $\bar{B}$ value and $\bar{W}$ are plotted against $\bar{W}$ to produce an estimate of the average underestimate in $\bar{W}$ when it is sampled in different sky-cover conditions. There is little variation of the underestimate with $\bar{W}$; it is largest when only clear skies are sampled, but still generally less than 5 kg m^{-2}.

4. Discussion

a. Surface temperature effects

As mentioned above, a possible explanation for the variation of $\bar{W}$ with cloud cover is that cloudy skies tend to be associated with warmer weather. To test this hypothesis, we compared seasonal mean surface temperature $\bar{T}$ for the four cloud-cover categories. An index of the temperature difference between clear and cloudy days is D_T, where

$$D_T = \bar{T}_{CLR} - \frac{N_{SCT}\bar{T}_{SCT} + N_{BKN}\bar{T}_{BKN} + N_{OVC}\bar{T}_{OVC}}{N_{SCT} + N_{BKN} + N_{OVC}}. \tag{7}$$

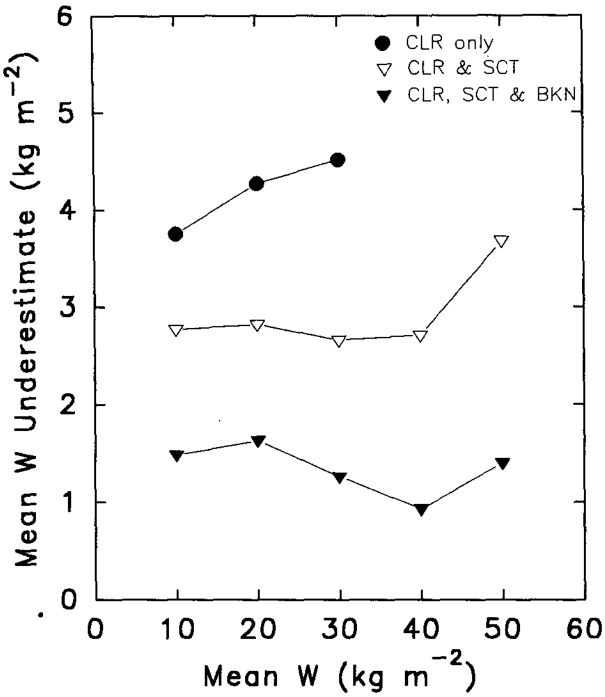

FIG. 5. Mean underestimates of mean column water vapor content, $\bar{W}$, for three sets of sky-cover sampling limitations.

If clear days are typically cooler than cloudy, D_T is negative, which is indeed the case at a few stations for some seasons. At Lake Charles and Washington Dulles, $\bar{T}$ under clear skies was 2° to 7°C lower than under cloudy skies in all seasons, with D_T generally lowest (more negative) in the colder seasons. This is probably related to the early morning observation time; nighttime cloud cover would lead to higher minimum temperatures than under clear skies. At London, Moosonee, and Jokioinen, D_T was −7° to −9°C in winter, but in summer D_T values are positive. The negative wintertime values at the stations can be understood in terms of the airmass argument, in which warm moist air masses are associated with higher cloud cover than cold dry air masses.

However, at all the other stations (except those with no CLR observations, so D_T could not be computed) D_T is positive (ranging from 1° to 7°C) in all seasons, because $\bar{T}$ decreases with cloud cover at most stations. Clear, dry days tend to be warmer than cloudy humid days. Thus, in general, the variation of $\bar{W}$ with cloud cover is not simply due to $\bar{T}$ variations.

b. Effects of radiosonde biases

The dependence of $\bar{W}$ on cloudiness noted above must be placed in the context of the dependence of radiosonde humidity measurement errors on cloudiness. To the extent that systematic biases or time lags in temperature or humidity measurements by radiosondes are affected by clouds, our estimates of $\bar{B}_0$, $\bar{B}_4$, and $\bar{B}_7$ will be misleading. And since different stations used different radiosonde types, the effects may vary from station to station.

For example, the U.K. Meteorological Office radiosonde used at Crawley during the three-year period of this analysis carried a goldbeater's skin hygrometer which is known to be biased low in clouds; the sensor rarely yields relative humidity (RH) values near 100% (Nash and Schmidlin 1987). Thus, we might expect the B values at Crawley to be an underestimate because $\bar{W}$ in cloudy skies, and therefore $\bar{W}_{ALL}$, are probably underestimated. However, the sensor is also biased high at low RH values (Nash and Schmidlin 1987), which may cause $\bar{W}_{CLR}$ and therefore B values, especially B_0, to be overestimated. How these opposing effects interact is difficult to estimate.

The radiosondes used at the stations operated by the United States and Canada carry a carbon hygristor. In the United States, the algorithm used to convert the radiosonde signal to RH rarely gives values above 95% (Schwartz and Doswell 1991), so B values are likely to be underestimated at the seven stations run by the United States, again because W is probably underestimated in the saturated or near-saturated conditions in clouds. [On the other hand at Midway, Liu et al. (1991) found frequent reports of 100% RH.] In Canada, the algorithm was changed in 1983 (G. Klein 1992, personal communication), so this problem should not apply to Moosonee data.

Four of the stations, Singapore, Athens, de Bilt, and Jokioinen, used the Finnish Vaisala radiosondes, which carry a thin film capacitive humidity sensor. This sensor has been shown to become wet in clouds and remain wet even above cloud top (Nash and Schmidlin 1987). This effect would tend to introduce a high bias in $\bar{W}_{ALL}$, which would cause B values to be overestimated.

These tendencies are *not* consistent with the B values in Table 2. Of the five tropical stations, Singapore's B values are consistently lower than the American stations' values. Athens, too, has lower B values than American stations at comparable latitudes. Thus we do not see patterns in the B values that are at all correlated with instrument type. This suggests that the instrument biases discussed above are not very important in determining B values, but that local variations in the way W varies with cloudiness dominate.

c. Summary of clear-sky bias

The $\bar{B}$ ratios defined and calculated above can be interpreted as estimates of the bias in climatologies limited to clear-sky or partly cloudy-sky observations. For example, if a particular W sensing system is only able to operate in completely clear skies, then $\bar{B}_0$ is an estimate of the reduction in $\bar{W}$ from that system compared to the true $\bar{W}$. If a sensor can determine W in partly cloudy skies, then the bias will depend on the minimum fractional amount of clear sky in the target area required to obtain a W value. In some cases, where the target area is larger than the satellite sensor footprint (i.e., a high-resolution field of view), a single cloud-free footprint area in a much larger target area might allow determination of W (A. Gruber 1992, personal communication). In that case, only OVC skies pose a problem, and $\bar{B}_7$ estimates the bias in the climatology. The ratio $\bar{B}_4$ estimates the bias in climatologies based on data in which 50% clear sky in the target region would suffice to make W measurements. Of course, these estimates do not take into account such factors as the size of the target area versus the area "sampled" by a human observer, the effect of cloud opacity on the measurements, or the effect of slant angles.

Because there are regional differences in the apparent bias and seasonal differences at each station examined, it would be dangerous to extrapolate from our small sample to universal rules. Nevertheless, the data do give an estimate of the variations in this bias that might be encountered around the globe.

In the tropics, because of the paucity of clear-sky observations, it is difficult to provide quantitative estimates of the bias in $\bar{W}$ climatologies based only on clear-sky observations except to say it is probably a slight underestimate of the true mean. If partly cloudy-sky observations are used, the underestimate is about 10% to 15%. In higher-latitude continental areas the bias due to using only CLR observations (B_0) can range from about 25% to 50% in winter, and about 5% to 25% in summer, but again there were few clear, summer observations at some stations in our sample. By adding SCT (and BKN) observations to the climatology, the bias is generally diminished, and the bias is larger in winter than summer (only San Juan is an exception).

There were only 15 stations examined for this preliminary study and it bears repeating that the ratios reported here are but guidelines. Examining these ratios in a wider variety of climates and latitudes could permit better estimates of the clear-sky bias in column water vapor estimates.

5. Conclusions

Climatological column water vapor content for clear skies has been shown to be significantly lower than for cloudy skies. The magnitude of the difference is smaller in tropical regions than at midlatitude stations, where the clear-sky bias, quantified by the index B_0, is largest in winter. The variation in column water content with cloud cover is not due simply to variations in surface temperature. Biases in radiosonde instruments do not explain the variation in B values from station to station.

The B values developed here can be helpful in estimating the bias in water vapor climatologies based on clear-sky measurements. In addition, they may be useful in attempts to employ $\bar{W}$ climatologies that are *not* influenced by cloud cover, such as those produced from passive microwave observations (e.g., Prabhakara et al. 1982), in studies of the greenhouse effect of water vapor. Some such studies (e.g., Stephens and Greenwald 1991a,b; Duvel and Bréon 1991) have relied on monthly $\bar{W}$ statistics to determine the clear- and cloudy-sky greenhouse effect. In some methods, there is an implicit assumption that $\bar{W}$ is approximately the same in clear and cloudy skies (Cess et al. 1992), which, as this analysis shows, is not always a good assumption. The effect of cloud cover on $\bar{W}$ may need to be considered in estimating the magnitude of the water vapor greenhouse effect. Similarly, to determine the sign and magnitude of cloud radiative feedbacks accurately, the simultaneous effects of water vapor variations should be distinguished. We hope that the results presented here will assist in those efforts.

Acknowledgments. We thank Tom Ross and Neal Lott of the National Climatic Data Center, Research Customer Servicing Group, for making the DATSAV2 Surface Climatic Database available, Arnold Gruber of NOAA/NESDIS for helpful discussions, and Nina Zaitseva of the Central Aerological Observatory, Moscow, for bringing the work of L. P. Burova to our attention. This work was supported in part by the NOAA Climate and Global Change Program.

REFERENCES

Burova, L. P., 1988: Modern variations of integral water vapor content in the Arctic atmosphere. *Arctic Climate Monitoring,* A. J. Veskresensky, Ed., Gydrometeoizdat, 69–76.

Cess, R. D., G. L. Potter, W. L. Gates, J.-J. Morcrette, and L. Corsetti, 1992: Comparison of general circulation models to earth radiation budget experiment data: Computation of clear-sky fluxes. *J. Geophys. Res.,* **97,** 20 421–20 426.

Duvel, J. Ph., and F. M. Bréon, 1991: The clear-sky greenhouse effect sensitivity to a sea surface temperature change. *J. Climate,* **4,** 1162–1169.

Liu, W. T., W. Tang, and P. P. Niiler, 1991: Humidity profiles over the ocean. *J. Climate,* **4,** 1023–1034.

Nash, J., and F. J. Schmidlin, 1987: WMO International Radiosonde Intercomparison (U.K., 1984, U.S.A., 1985) Final Report, *WMO/TD-No. 195,* World Meteorological Organization, Instruments and Observing Methods Report No. 30, 103 pp. [Case Postale No. 2300, CH-1121, Geneva 2, Switzerland.]

NASA, 1991: The role of water vapor in climate: A strategic research plan for the proposed GEWEX Water Vapor Project (GVaP). D. O'C. Starr and S. H. Melfi, Eds., NASA CP-3120, 50 pp. [International GEWEX Project Office, 409 3rd St. SW, Washington, DC 20024.]

Peixoto, J. P., and A. H. Oort, 1992: *Physics of Climate.* American Institute of Physics, 520 pp.

Prabhakara, C., H. D. Chang, and A. T. C. Chang, 1982: Remote sensing of precipitable water over the oceans from *Nimbus-7* microwave measurements. *J. Appl. Meteor.,* **21,** 59–68.

Rossow, W. B., and A. A. Lacis, 1990: Global, seasonal cloud variations from satellite radiance measurements. Part II: Cloud properties and radiative effects. *J. Climate,* **3,** 1204–1253.

Schwartz, B. E., and C. A. Doswell III, 1991: North American rawinsonde observations: Problems, concerns, and a call to action. *Bull. Amer. Meteor. Soc.,* **72,** 1885–1896.

Stephens, G. L., and T. J. Greenwald, 1991a: The earth's radiation budget and its relation to atmospheric hydrology: 1. Observations of the clear sky greenhouse effect. *J. Geophys. Res.*, **96**, 15 311–15 324.

——, and ——, 1991b: The earth's radiation budget and its relation to atmospheric hydrology: 2. Observations of cloud effects. *J. Geophys. Res.*, **96**, 15 311–15 324.

Tselioudis, G., W. B. Rossow, and D. Rind, 1992: Global patterns of cloud optical thickness variations with temperature. *J. Climate*, **5**, 1484–1495.

USAFETAC, 1986: *Climatic Database Users Handbook No. 4*, DATSAV2 Surface (Unclassified), U.S. Air Force Environmental Technical Applications Center, USAFETAC/UH-86/004. 6 pp. plus appendixes.

Warren, S. G., C. J. Hahn, J. London, R. M. Chervin, and R. L. Jenne, 1986: *Global Distribution of Total Cloud Cover and Cloud Type Amounts over Land.* U.S. Dept. of Energy, and National Center for Atmospheric Research, DOE/ER-60085-H1, NCAR/TN-273+STR, 29 pp. and 199 maps.

——, ——, ——, ——, and ——, 1988: *Global Distribution of Total Cloud Cover and Cloud Type Amounts over the Ocean.* U.S. Dept. of Energy, and National Center for Atmospheric Research, DOE/ER-0106, NCAR/TN-317+STR, 42 pp. and 107 maps.

WMO, 1991: *Manual on Codes, Vol. I International Codes, Part A Alphanumeric Codes.* 1988 edition, Suppl. No. 2 (VI. 1991), WMO-No. 306, World Meteorological Organization.